

The Mass and Radius of the Neutron Star in the Bulge Low-Mass X-ray Binary KS 1731–260

Feryal Özel¹, Andrew Gould², and Tolga Güver¹

¹*University of Arizona, Department of Astronomy, 933 N. Cherry Ave., Tucson, AZ 85721, USA; fozel@email.arizona.edu, tguver@email.arizona.edu*

²*Department of Astronomy, Ohio State University, 140 W. 18th Ave., Columbus, OH 43210, USA; gould@astronomy.ohio-state.edu*

ABSTRACT

Measurements of neutron star masses and radii are instrumental for determining the equation of state of their interiors, understanding the dividing line between neutron stars and black holes, and for obtaining accurate statistics of source populations in the Galaxy. We report here on the measurement of the mass and radius of the neutron star in the low-mass X-ray binary KS 1731–260. The analysis of the spectroscopic data on multiple thermonuclear bursts yields well-constrained values for the apparent angular area and the Eddington flux of the source, both of which depend in a distinct way on the mass and radius of the neutron star. The binary KS 1731–260 is in the direction of the Galactic bulge, allowing a distance estimate based on the density of stars in that direction. Making use of the Han & Gould model, we determine the probability distribution over the distance to the source, which is peaked at 8 kpc. Combining these measurements, we place a strong upper bound on the radius of the neutron star, $R \leq 12$ km, while confining its mass to $M \leq 1.8 M_{\odot}$.

Subject headings: stars: neutron — X-rays: binaries — stars: individual (KS 1731–260)

1. Introduction

A direct probe of the equation of state of cold, ultradense matter is the measurement of the radii of neutron stars, whose cores are comprised of the densest matter in the current universe. Radii measurements can distinguish between a variety of interior compositions, as well as the strength of the many-body nuclear force (Lindblom 1992; Lattimer & Prakash 2001; Read et al. 2009; Özel & Psaltis 2009). In addition, the mass distribution of neutron stars can give insights to the outcomes of supernova explosions and evolutionary tracks in

binaries. If sufficiently high, a mass measurement can also lead by itself to constraints on the composition and the interactions of the interior (Demorest et al. 2010; Özel et al. 2010a).

While precise mass measurements of neutron stars have been possible for decades, significant progress in the determination of radii of neutron stars has been made only recently. There are, by now, a handful of neutron stars for which both a radius and a mass measurement have been achieved. Some of these spectroscopic observations have been carried out during the quiescent episodes of accreting sources that reside in globular clusters (Rutledge et al. 2001; Heinke et al. 2006; Webb & Barret 2007; Guillot et al. 2010). They have led to significant, albeit correlated, constraints in the mass and radius of neutron stars.

Another way to measure the neutron star mass and radius is through a combination of spectroscopic phenomena observed from their surfaces during thermonuclear X-ray bursts (van Paradijs 1979; Özel 2006). The repeated high count-rate bursts allow a measure of the apparent angular area of the neutron star over a wide range of temperatures using time-resolved spectra. Furthermore, very luminous X-ray bursts (called photospheric radius expansion, or PRE, bursts) cross the local Eddington flux at the neutron star surface and allow us to obtain a measure of the neutron star mass (as corrected for general relativistic effects). Combined with the distance measurement to the source, these quantities can be converted into independent measurements of the neutron star mass and radius. This approach led to the determination of the masses and radii of several neutron stars (Özel et al. 2009; Güver et al. 2010a, b) and enabled the measurement of the pressure of neutron star matter above nuclear saturation density (Özel et al. 2010b).

In this paper, we place strong constraints on the mass and radius of KS 1731–260 based on the analysis of thermonuclear bursts observed with the Rossi X-ray Timing Explorer. The transient X-ray burster KS 1731–260 was discovered in 1989 during observations with the TTM/Kvant telescope on board the Mir station (Sunyaev et al. 1990). Three Type I bursts were seen during the immediate follow-up observations, confirming the presence of a neutron-star in this X-ray binary. RXTE detected a total of 24 Type-I bursts from KS 1731–260, which allow a systematic study of the spectra obtained during the bursts and the measurement of the surface area and the Eddington limit of this neutron star (Galloway et al. 2008; Güver et al. 2010c, d).

In order to convert the measurement of the apparent angular area and Eddington flux from the surface of a neutron star into a measurement of its mass and radius, we need an estimate of the distance to the source. In earlier work, we used sources in globular clusters with known distances (Özel et al. 2009; Güver et al. 2010b) or measured the source distance using the method of red clump stars (Güver et al. 2010a). In this paper, we use the fact that KS 1731–260 lies within the Galactic bulge, which has a limited spatial extent in the

Galaxy. Even though the further localization of the source within the bulge is not easy to achieve, it nevertheless allows us to place a strong upper bound on the mass and radius of the neutron star.

In Section 2, we present the constraints on the distance to KS 1731–260. In Section 3, we summarize the results from the analysis of the spectra of thermonuclear bursts from this source and show the resulting constraints on its mass and radius. In Section 4, we compare these measurements to other existing mass-radius measurements.

2. The Distance to KS 1731–260

KS 1731–260 lies at galactic coordinates $(l, b) = (1.06, 3.65)$, i.e., almost exactly at the position of Baade’s window (reflected in the Galactic plane). Its position toward the bulge allows an estimate of its distance based on the distribution of stars in that direction. Having no prior information on the distance to KS 1731–260, we will assume that the likelihood that it resides at a given distance D is proportional to the number density of stars along the line of sight to the bulge at that distance.

For the stellar distribution along the line of sight we adopt the model of Han & Gould (2003), which is based primarily on star counts, and, without any adjustment, reproduces the microlensing optical depth measured toward Baade’s window. For the bulge, Han & Gould (2003) normalize the “G2” K-band integrated-light-based bar model of Dwek et al. (1995) using star counts toward Baade’s window from Holtzman et al. (1998) and Zoccali et al. (2000). For the disk, they incorporate the model of Zheng et al. (2001), which is a fit to star counts. In this model, there is a 1 kpc hole at the center of the Galactic disk, since this material would have gone into the Galactic bulge according to the standard picture of pseudo-bulge formation. We normalize the distance scale to a Galactocentric distance of $R_0 = 8.0 \pm 0.4$ kpc (Yelda et al. 2010). The position of the source, being almost exactly at the position of Baade’s window (reflected in the Galactic plane), minimizes the extrapolation from calibrating star counts to the adopted model.

In Figure 1, we plot the stellar distribution along the line of sight to KS 1731–260, which we then take to be equal to the likelihood of the source distance. The dotted lines show the disk and bulge contributions separately, while the solid line shows the total likelihood for a distance to the Galactic center of 8.0 kpc. The dashed line shows the likelihood of the distance to KS 1731–260 when a Gaussian uncertainty of 0.4 kpc has been incorporated to the distance to the Galactic center. It is evident from the dashed curve that the details of the prescription for the 1 kpc hole in the Galactic disk are not important. The latter likelihood,

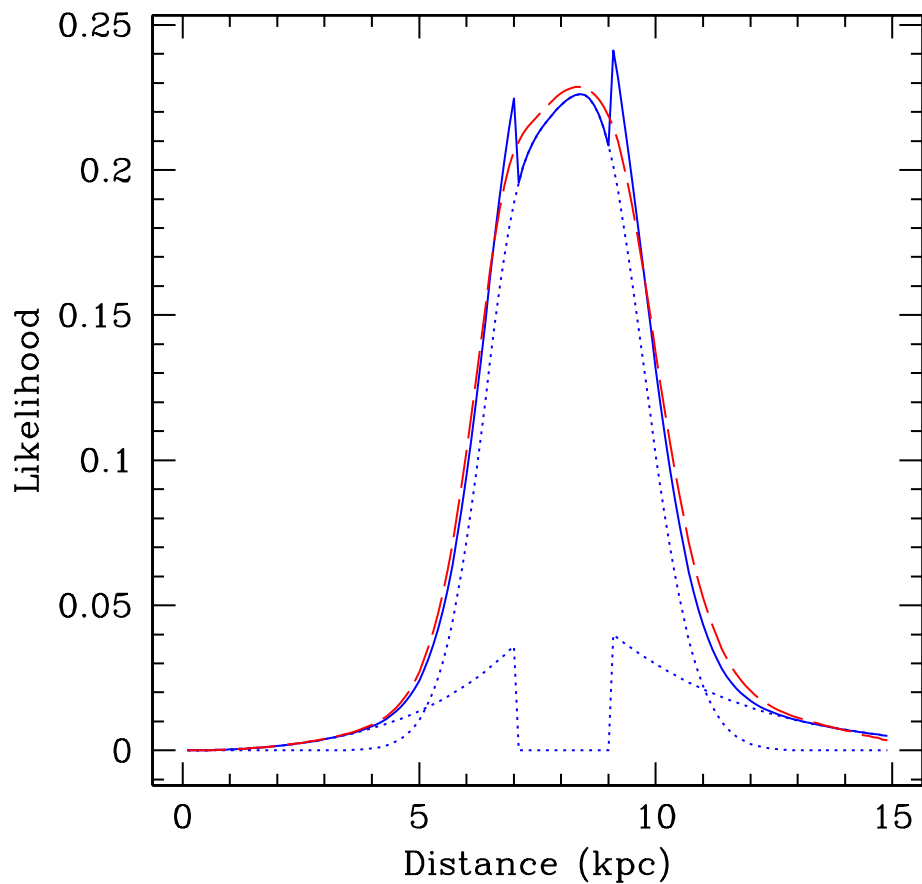


Fig. 1.— The solid line shows the likelihood of the distance to KS 1731–260, which we have taken to be proportional to the number density of stars along the line of sight to the source, at each given distance, for an assumed distance to the Galactic center of 8.0 kpc. The dotted lines show the disk and bulge components of this distribution. The dashed line shows the total likelihood of the distance to KS 1731–260 when a Gaussian uncertainty of 0.4 kpc has been incorporated to the distance to the Galactic center.

which we use hereafter, indicates that the source most probably lies at $5 \text{ kpc} < D < 11 \text{ kpc}$.

3. Determination of the Neutron Star Mass and Radius from X-ray Burst Spectroscopy

RXTE observed KS 1731–260 for a total of 483 ks until June 2007. We reported in Güver et al. (2010c) the systematic analysis of the 24 bursts detected in this time period. All of the details related to the extraction of the spectra, detector response, background subtraction, and the spectral fitting are discussed in Güver et al (2010c). We only summarize here the results of the analysis of the time-resolved continuum spectra in order to utilize them for the mass and radius determination of the neutron star in this binary.

The 24 bursts we use here met our requirement that the persistent flux prior to the burst was $< 10\%$ of the peak burst flux, which minimizes uncertainties related to background subtraction. We analyzed a total of 1309 spectra from these bursts, out of which 1240 spectra (98%) gave acceptable values of reduced χ^2 . We measured the evolution of the flux, the temperature, and the angular size using the spectra obtained from 0.25, 0.5, or 1 s integrations during each burst. The bursts follow highly reproducible tracks on the flux-temperature diagram, as is shown in Figure 2. The slight decline in the normalization at very low fluxes is consistent with the expected increase of the color correction factor at low temperatures. Incorporating this trend as a systematic uncertainty, Güver et al. (2010c) reported an apparent angular area of $A = 88.4 \pm 5.1 \text{ (km/10 kpc)}^2$, which corresponds to a radius of $9.4 \pm 0.3 \text{ (km/10 kpc)}$ during the cooling tails of bursts. The quoted uncertainty in the radius includes statistical and systematic uncertainties. The apparent angular area depends on the stellar parameters according to

$$A = \frac{R^2}{D^2 f_c^4} \left(1 - \frac{2GM}{Rc^2} \right)^{-1}, \quad (1)$$

where f_c is the color correction factor.

Two out of the 24 bursts from KS 1731–260 showed clear evidence of photospheric radius expansion, where the photosphere in highly energetic burst events expands to many times the stellar radius, while the flux and temperature follow a characteristic evolution (see Güver et al. 2010d). We measured the Eddington flux in these events at the touchdown moment when the photosphere returns to the stellar surface, as indicated by a maximum in the temperature and a minimum in the inferred area (as in Özel et al. 2009 and Güver et al. 2010d). For KS 1731–260, we found an average touchdown flux of $(4.45 \pm 0.12) \times 10^{-8} \text{ erg cm}^{-2} \text{ s}^{-1}$, where the quoted uncertainty is purely formal. Because in sources with larger number of

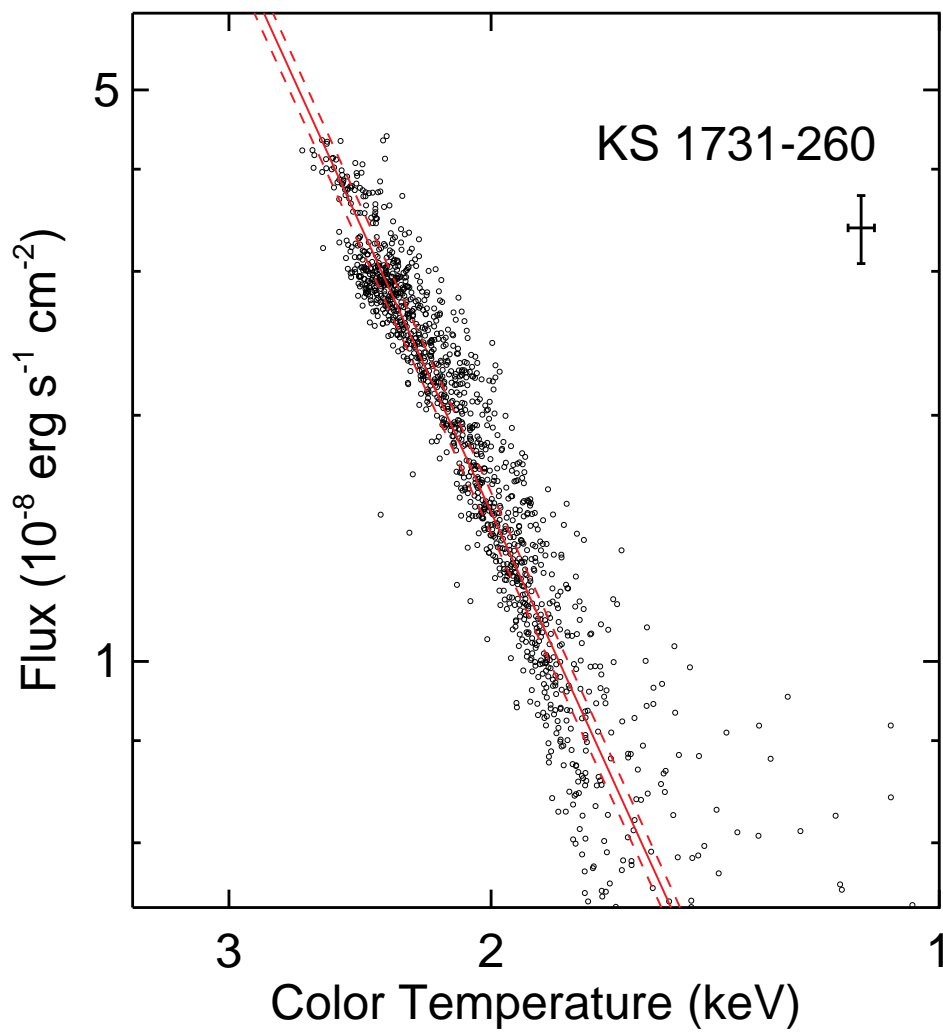


Fig. 2.— The evolution of the bolometric flux and the blackbody temperature during cooling tails of three thermonuclear X-ray bursts observed from KS 1731–260. The bursts follow the $L \propto T^4$ relation, which is indicated by the solid line.

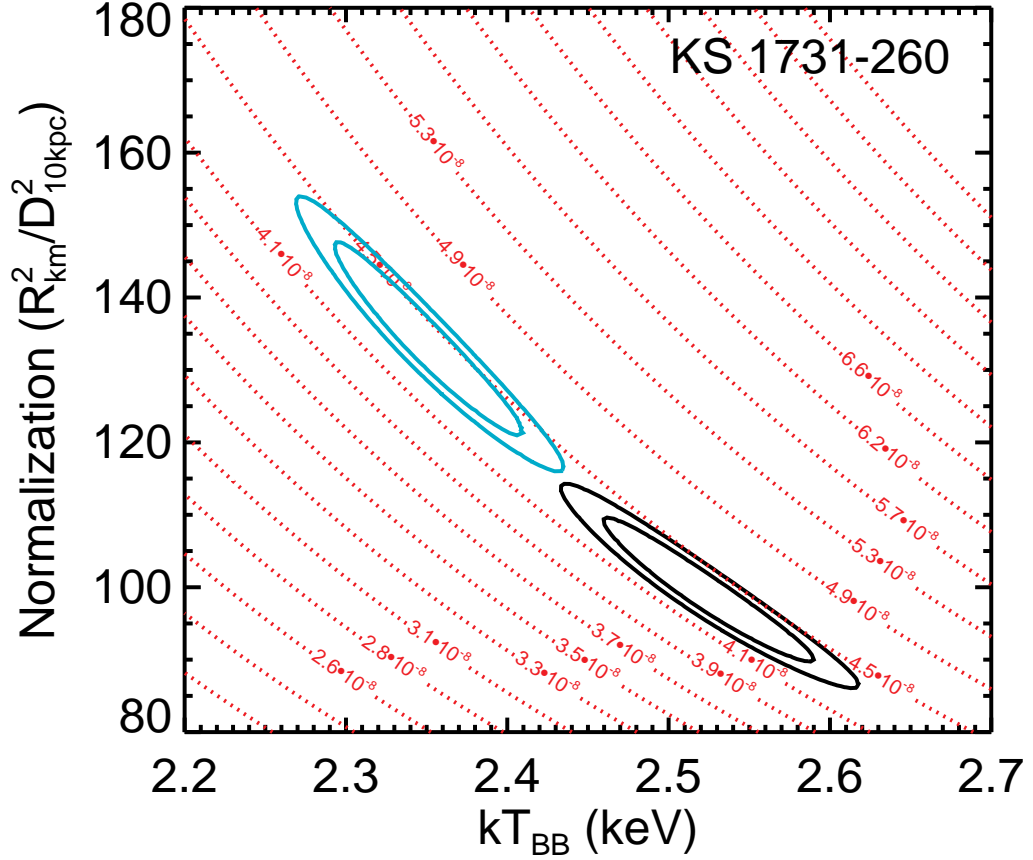


Fig. 3.— The confidence contours over the blackbody temperature and normalization during the touchdown moments of the two photospheric radius expansion bursts (in green and black, respectively) observed from KS 1731–260. The two bursts differ in both temperature and angular area, and they each have significant uncertainties in these variables, which are strongly correlated. However, when the distribution is projected onto Eddington flux (red curves), the result is quite consistent between the two bursts and well constrained.

photospheric radius expansion bursts we found systematic uncertainties of the order of $\sim 5\%$ in the touchdown flux, we assign hereafter a total uncertainty of $0.22 \times 10^{-8} \text{ erg cm}^{-2} \text{ s}^{-1}$ in order to be conservative. The touchdown flux depends on the stellar parameters as

$$T_{\text{td}} = \frac{GMc}{k_{\text{es}}D^2} \left(1 - \frac{2GM}{Rc^2} \right)^{1/2}, \quad (2)$$

where G is the gravitational constant, c is the speed of light, and k_{es} is the opacity to electron scattering.

We assign independent probability distribution functions to the distance $P(D)dD$, the touchdown flux $P(F_{TD})dF_{TD}$, and apparent angular area normalization $P(A)dA$ based on the measurements and the distance estimate discussed above. We take the probability distributions over the touchdown flux and the apparent angular area to be Gaussian. Converting the Eddington limit and the apparent angular area to a mass-radius measurement requires a prior knowledge of the hydrogen mass fraction X in the atmosphere and a model for the color correction factor f_c . In the absence of any information on the composition of the accreted material for KS 1731–260, we take a box-car distribution for X that covers the range 0–0.7. The color correction factor, on the other hand, is obtained from modeling the hot atmospheres of accreting, bursting neutron stars (e.g., Madej, Joss, & Rozanska 2004). We take the box-car probability distribution centered at $f_{c0} = 1.35$ and a width $\Delta f_c = 0.05$ that is appropriate for a thermal flux in the range between $\approx 1\% - 50\%$, which is seen in the cooling tails of bursts (see Güver et al. 2010b, 2010c for a detailed discussion).

We calculate the probability distribution over the neutron star mass and radius as in Güver et al. (2010a). Note that we have corrected here an error in the Equation (5) of Özel et al. (2009) where the term $7GM/Rc^2$ should read $8GM/Rc^2$. Figure 4 (left panel) shows the 68% and 95% confidence levels for the mass and the radius of the neutron star in KS 1731–260. Although the observed apparent angular area and the touchdown flux are consistent with a range of masses and radii for the neutron star, they nevertheless provide a strong upper bound of $R < 12 \text{ km}$ and $M < 1.8M_{\odot}$. In Figure 4, we also identify the astrophysically relevant range of neutron star masses $M > 1.2M_{\odot}$ and show the combined constraints as filled contours. The allowed range of neutron star radii is inconsistent with equations of state that predict large neutron star radii, $\sim 12 - 15 \text{ km}$. This is in agreement with the earlier spectroscopic measurements of radii in bursting neutron stars (Özel et al. 2009; Güver et al. 2010a, b) as well as the quiescent neutron stars in globular clusters (Webb & Barret 2007; Guillot et al. 2010).

When performing parameter estimation in models within a Bayesian framework, two concerns often arise. First, there is no universally accepted measure of goodness-of-fit, which makes it difficult to assess whether data sets that are used to estimate the parameters are

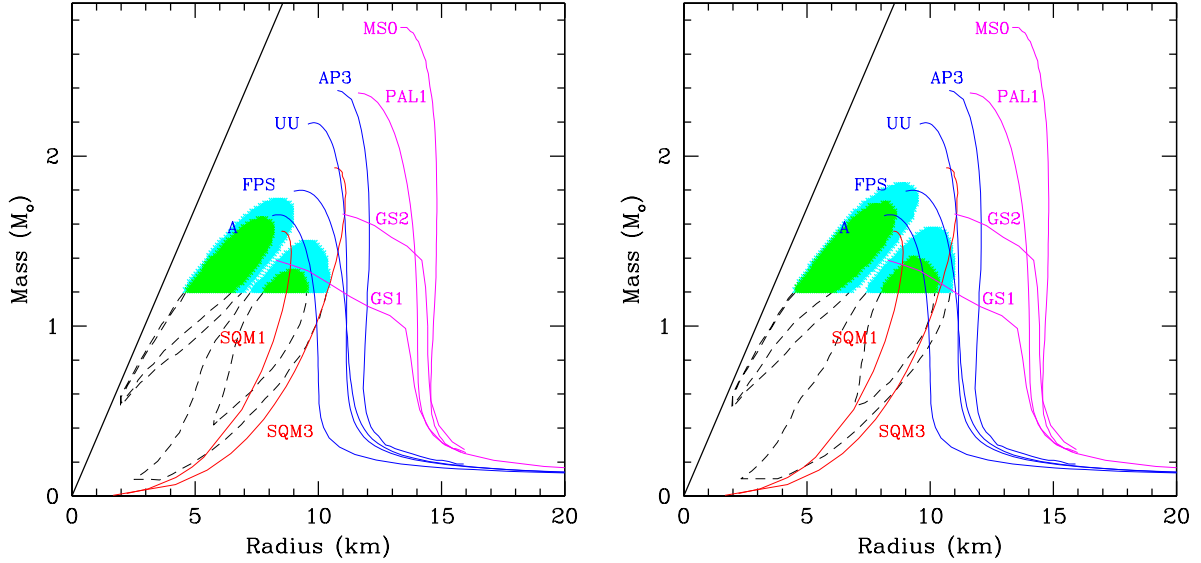


Fig. 4.— *(Left)* The 68% and 95% confidence contours for the mass and radius of the neutron star in KS 1731–260. The astrophysically relevant range of masses $M > 1.2M_{\odot}$ are shown as filled contours. The representative mass-radius relations for a select number of equations of state are also shown and include multi-nucleonic ones (A, FPS, UU, AP3), equations of state with condensates (GS1-2), strange stars (SQM1, SQM3), and meson-exchange models (MS0). The black line indicates the black hole event horizon. The descriptions of the various equations of state and the corresponding labels can be found in Lattimer & Prakash (2001) and Cook, Shapiro & Teukolsky (1994). *(Right)* The 68% and 95% confidence levels over neutron-star mass and radius calculated by using the maximum combined likelihood along lines of constant distance and hydrogen mass fraction rather than by integrating over these two nuisance parameters. The fact that these confidence levels are very similar to those shown in the left panel demonstrates that marginalization does not bias the results.

consistent with the model. Second, in models with more than two parameters, marginalizing (integrating) over the so-called nuisance parameters in Bayesian analysis in order to infer the parameters of interest can introduce biases. This is especially a concern when measurement uncertainties in different parameters differ widely from each other. In our case, the allowed logarithmic range of values over distance is significantly larger than the uncertainties over the touchdown flux and the apparent radius. These concerns have led Steiner et al. (2010) to explore a different, ad hoc, interpretation of the Eddington flux in their inference of the neutron star masses and radii.

In Figure 5, we show the contours in the mass-radius plane that correspond to each individual spectroscopic measurement, taking into account the 1σ ranges in the measured quantities but fixing the distance to a representative value of 7 kpc, which is within the region of highest likelihood (see Fig. 1) and in the range of distances most favored by the data. The two sets of contours intersect with each other within their 1σ levels and overlap with the combined confidence contours over mass and radius. Even though this is not a quantitative measure of goodness-of-fit, it shows the self-consistency of the theoretical framework with the data.

In order to address the second concern about the effect of marginalizing over distance, we performed the following test. We calculated the likelihood over mass and radius by using the *maximum* of the combined likelihood along lines of constant distance and constant hydrogen mass fraction X , instead of integrating over these two parameters. We show in the right panel of Figure 4 the resulting confidence contours over mass and radius. The result is very similar to that shown in the left panel of Figure 4, demonstrating that the marginalization over the two most uncertain parameters, namely distance and the hydrogen mass fraction, does not bias the mass and radius measurement.

4. Conclusions

We used the spectroscopic measurements of the apparent angular area and the Eddington flux during thermonuclear X-ray bursts from KS 1731–260 to measure its mass and radius. We place a strong upper bound on the radius of $R < 12$ km and confine the mass to $M < 1.8M_{\odot}$. This measurement challenges equations of state that predict radii larger than ~ 12 km.

We also explored whether, within the Bayesian parameter estimation approach, 1. the theoretical framework and the data sets used here are self-consistent and 2. the integration over the nuisance parameters introduces biases in the confidence limits over the neutron star

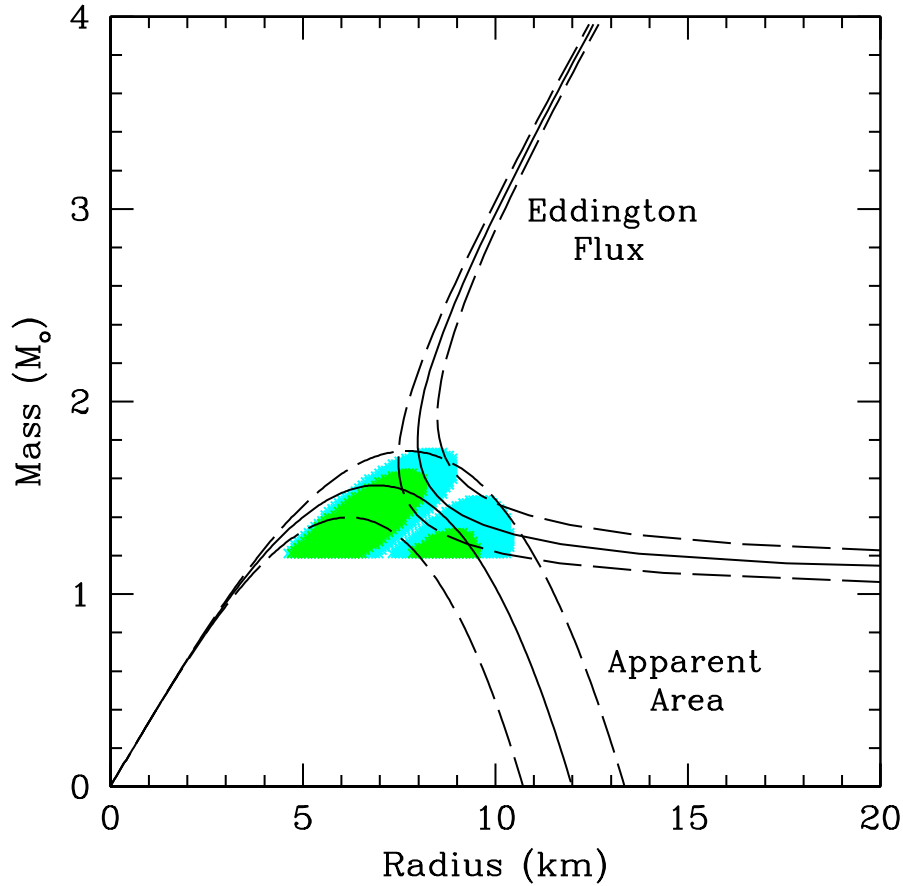


Fig. 5.— The contours in the mass-radius plane that correspond to the measurement of the Eddington flux and the apparent radius for a representative distance of 7 kpc. The dashed lines reflect the 1σ errors on the measured quantities and model parameters. The fact that the two sets of contours intersect at the location of the confidence limits shown in the left panel of Figure 4 and overplotted here (filled contours) demonstrate the consistency of the model with the data.

mass and radius. We found that for a highly likely value of the distance, the contours in the mass-radius plane that correspond to the apparent radius and the Eddington limit are consistent with each other and with the confidence contours over mass and radius within 1σ . Moreover, we showed that considering the most likely configuration for each value of the distance and the hydrogen mass fraction, as opposed to integrating over these two parameters, leaves the results largely unaffected. These results justify our identification of the touchdown point for the measurement of the Eddington flux and our conclusion that the apparent angular area during the cooling tail of the burst corresponds to the entire neutron star surface.

This work was supported in part by NASA ADAP grant NNX10AE89G and Chandra Theory grant TMO-11003X. AG was supported by NSF grant AST-0757888. We thank Andrew Steiner for pointing out an error in a numerical factor in our earlier calculation of the Jacobian transformation. We thank Dimitrios Psaltis for a careful reading of the manuscript.

REFERENCES

- Cook, G. B., Shapiro, S. L., Teukolsky, S. A. 1994, *ApJ*, 424, 823
- Demorest, P. B., Pennucci, T., Ransom, S. M., Roberts, M. S. E., & Hessels, J. W. T. 2010, *Nature*, 467, 1081
- Dwek, E., et al. 1995, *ApJ*, 445, 716
- Galloway, D.K., Muno M. P., Hartman J. M., Psaltis D., Chakrabarty D. 2008, *ApJS*, 179, 360
- Guillot, S., Rutledge, R. E., & Brown, E. F. 2010, arXiv:1007.2415
- Güver, T., Özel, F., Cabrera-Lavers, A., & Wroblewski, P. 2010a, *ApJ*, 712, 964
- Güver, T., Wroblewski, P., Camarota, L., Özel, F. 2010b, *ApJ*, 719, 1807
- Güver, T., Psaltis, D., & Özel, F. 2010c, *ApJ*, submitted
- Güver, T., Özel, F., & Psaltis, D. 2010d, *ApJ*, submitted
- Han, C. & Gould, A. 2003, *ApJ*, 592, 172
- Heinke, C. O., Rybicki, G. B., Narayan, R., & Grindlay, J. E. 2006, *ApJ*, 644, 1090

- Holtzman, J.A., Watson, A.M., Baum, W.A., Grillmair, C.J., Groth, E.J., Light, R.M., Lynds, R., & O’Neil, E.J., Jr. 1998, *AJ*, 115, 1946
- Lattimer, J.M. & Prakash M., 2001, *ApJ*, 550, 426
- Madej, J., Joss, P. C., & Rózańska, A. 2004, *ApJ*, 602, 904
- Özel, F. 2006, *Nature*, 441, 1115
- Özel F., Güver T., & Psaltis D., 2009, *ApJ*, 693, 1775
- Özel, F. & Psaltis, D. 2009, *Phys. Rev. D*, 80, 103003
- Özel, F., Psaltis, D., Ransom, S., Demorest, P., & Alford, M. 2010, *ApJ*, 724, L199
- Rutledge, R. E., Bildsten, L., Brown, E. F., Pavlov, G. G., Zavlin, V. E., & Ushomirsky, G. 2002, *ApJ*, 580, 413
- Steiner, A. W., Lattimer, J. M., & Brown, E. F. 2010, *ApJ*, 722, 33
- van Paradijs, J. 1979, *ApJ*, 234, 609
- Webb, N. A. & Barret, D. 2007, *ApJ*, 671, 727
- Yelda, S., Ghez, A.M., Lu, J.R., Do, T., Clarkson, W., & Matthews, K. 2010, *The Galactic Center: A Window on the Nuclear Environment of Disk Galaxies*, eds. M. Morris, D. Q. Wang and F. Yuan, in press
- Zheng, Z., Flynn, C., Gould, A., Bahcall, J.N., & Salim, S. 2001, *ApJ*, 555, 393
- Zoccali, M., Cassisi, S., Frogel, J.A., Gould, A., Ortolani, S., Renzini, A., Rich, R.M., & Stephens, A.W. 2000, *ApJ*, 530, 418